Created a Realistic Virtual Human Body Model through the Radius Distance Free Form Deformation and Anthropometric Measurement

Sheng-Fuu Lin [#1], Shih-Che Chien[#2]

Institute of Electrical Control Engineering
National Chiao Tung University
1001 University Road, Hsinchu City, Taiwan 300, ROC

[1] sflin@mail.nctu.edu.tw

[2] Shihche.chien@gmail.com

***Abstract*— Nowadays the interest in creating 3D real humans is one of the most challenging problems and a topic of great interest and has been investigated within different research activities in the last decade. A methodology is proposed for creating a computer generated virtual mannequins through the individual anthropometric measurement. The example based deformation is performed to preserve more details and save more processing time. For more approximated to the real body, the human body is divided into several parts for deformation via each anthropometric measurement. For seamless body shape, the Skeleton link frame and several key joints are adopted to make a smoothing connection of each divided part.**

The radius distance free form deformation is the extended cylinder free form deformation and to be the method for deformation through each corresponding anthropometric measurement in each part. In this paper, the example based 3-D object deformation is used and provides a proper way to create a virtual mannequin with lower constrains. So the virtual mannequins are then adjusted by using the measurement of the nearest cluster example model. In this way, the realistic accurate virtual mannequins are created.

***Keywords*— Include at least 5 keywords or phrases**

I. INTRODUCTION

In recent years, the research of computer graphic is mostly focused on achieving realism in virtual environment. Particularly, the functional animation of human body is developed to simulate the action conformed to anatomical properties. The adjustment of 3-D object models to fit real world measurements provides an important challenge to the research. In particular, the existing approaches of computer generated virtual human body (mannequins) usually do not sufficiently to model the complex and individual virtual mannequins. In other words, the virtual mannequins which do not reflect anthropometric realities are therefore not specific enough for commercial use.

Modelling a virtual mannequin has attracted more and more attention from both the research and industrial community in recent years. It is not longer fantasy to imagine that one can see the exclusive virtual mannequin basis on him/her anthropometric measurement in the 3-D virtual environment. Moreover, by advance animation algorithm and scene management, the exclusive virtual mannequin can do some actions as talking, walking…etc. In novel commercial activity, the virtual mannequin has many applications in e-commerce and garment design. Now a day, the most of people are accustomed to shop on website and have no chance to see the actual item which purchased on website before shipping arrive. So the number of goods being returned may be unacceptable high, especially in buying clothes. If the virtual mannequin belong to customer is available, the return rate of clothes purchased on website unfitness will be down.

Anthropometric measurement is used in order to establish the human body physical geometry, mass property, and strength capabilities. Anthropometry, name derived from the Greek arthropos and metrikos, is the study of human body measurements (height, weight, size, circumference, etc.) and its biomechanical characteristics.

Trough the use of manual measurements by domain experts [1], combined with precise optoelectronic measurement devices, an accurate anthropometric measurement can be obtained. Anthropometric measurement data is referred to a collection of physical dimensions of human body and aim to characterize the human body by a set.

There has been significant hardware development in computer graphics and laser scanning technology during the last three decades. With the operational ability improvement, the whole human body scanning and virtual body generation can be done, and furthermore, the extension commercial applications of 3-D body scanning and generation have been achieved in clothes selling [2]. The CAESAR [3] project is the first large scale 3-D anthropometry survey project and an international anthropometric survey that was carried out in the U.S., Italy, The Netherlands, and Canada. This project is sponsored by the U.S. Air Force and involves about 40 contributing multinational companies mainly from the transportation and the apparel industry. In CAESAR database [4], each individual scanned recorded 49 anthropometric measurements, including details such as the arm length, the waist circumference…etc, which represents a detail and accurately measured subset of the typical humane morphology, together with a 3-D body scan which maps these measurement. Although, the 3-D scanning and generated virtual model has high accuracy and preserve more information of human body shape, post processing the raw data takes too much time to get a final result.

The methodologies of human body deformation can be classified into three classes, creative, reconstruction, and example based. The methodologies of creating are always using the 3-D Computer Aided Design (CAD) programs to assist the designer for creation, as like 3DMax [5] and

MAYA [6]. The 3-D laser scanning method mentioned on past paragraph is also the one kind of creating method for human body deformation [7]. The method using CAD program assistance is not suitable for creating complexity human body object, because the 3-D full human object will contain with more than ten thousand triangle patch and twenty thousand vertexes. In addition to the substantial computing of 3-D scanning raw data, the scanning instruments and sophisticated operator are not available everywhere. So the 3-D scanning method can not be wildly used for some applications, especially for remote application. The deformation method of reconstruction is performed with instrument calibration and geometric feature analysis [8][9][10]. The common drawback of reconstruction method is the resolution of created object, because the geometric feature analyses are always sacrificed the pixels captured from the item. In generally, the reconstruction method is adapted for creating a 3-D object model for small items, and not for the big or complex surface item.

The example based deformation methods are the process of mapping some of vertices of the underlying model from one space to the other. Thus movement of vertex is closely associated with the moving of control points. The example based deformation is not only intuitive and easier to control, but also retained the benefit, including details and rich information 3-D human body object, of 3-D laser scanning creating method. Therefore, it is a very important concept in the object modelling and deformation fields.

The earlier researches of example based deformation starts with Barr's [11] work on parametric shapes which called super quadrics. The extended approach Scheepers [12] used similar parametric shapes to anatomically model the body muscle. Sederberg and Parry [13] proposed the Free Form Deformation (FFD) technique where a 3-D model embedded into a parallelepiped box, and deforming the box will also deform the underlying complex model. Chadwick [14] who added dynamic muscle effect on top of the skeleton with FFD technique to animate the human body model presented an absorbing application of FFD technique. Coquillart [15] proposed an extended version of the standard FFD method where non-parallel piped 3D lattices are used to include the irregular shapes for deformation.

The earlier researches about anthropometric modeling of the human body model are started by Grosso et al. [16], and then Azuola et al.[17] are also proposed a anthropometry based virtual human model. Human body model is segmented into groups according to joints and joint deformation is applied for animation. In Grosso's development, a human body model is segmented into 24 polyhedral geometric primitives with length, width and depth parameters. Jianhua [18] provided a new approach for body model representation. Jianhua divided the model into slices and a radius of each slice is scaled to achieve the partial deformation, as like muscular, for deformation effect. Jianhua [19] also extended this contour based representation of body model with metaballs [20]. Like cylindrical representation, metaballs are used for smooth and detailed modeling. Another approach for human body deformation is applying the sweep based method on the limbs [21] and full body [22]. In this approach each limb is approximated by swept based ellipsoid which changes its size as it moves through the limb. Transition from each joint, the ellipsoid changes its orientation through the new one, therefore, the virtual body can do some action according to the anatomical principals. As similar to sweep based deformation, Zhaoqi et al. [23] presented a Cross sectional representation of the body model to generate skeleton-driven deformations.

This paper is organized as follows. Section II describes the definition of human body model segmentation. The feature points, including connected node and associate location points, are used to locate the position of cutting plane, which is accessed for separating each part of human body. The method Radius Distance Deformation (RDD) is explained in section III. The cylinder coordinate system which is adopted in this paper is well used for human body deformation and the Radius Distance Deformation is also based on cylinder coordinate system. The relation function of human body anthropometric measurement and body model deformation are received from the prior calculation of the human body from TAIBBK database based on radius distance deformation. In the section IV, the Free Form Deformation (RD-FFD) is proposed and used to deform the example model with the anthropometric measurement. Through of these methods, the realistic virtual human bodies are created. The implementation of this approach is showed in section V. Section VI concludes this paper. The flowchart of this system illustrated in Fig. 1.

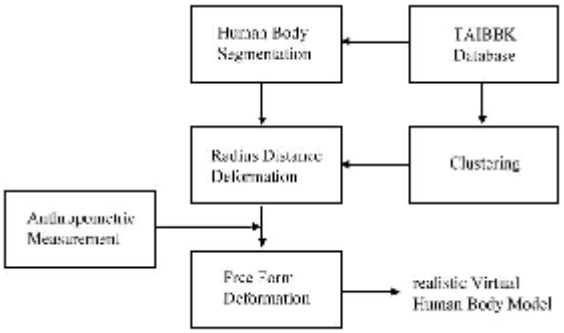

Fig. 1 The flowchart of this paper.

II. HUMAN BODY SEGMENTATION

In this section, the segmentation of human body is during the anatomical principals, thus the connect junction are always located at the some important joints, as like shoulder joint (connection of upper arm and torso) and elbow joint (connection of upper arm and forearm). The body is typically built as a series of nested Joints, each of which may have a Segment associated with it. At first, we will descript the skeleton frame which construct with skeletons and joints and well used to human body segmentation. The principle of body model segmentation is handed by the cutting plane which is created at the separated position, which is usually at the concern joints. The details of these methods will be explained in the follow paragraph.

A. Skeleton Frame

As the 3D application continues to grow, there will be an increasing need to represent human beings in virtual environments. The humanoid animation is wildly used in many fields especially in film industry. In this thesis, we are not only present a methodology for creating a realistic virtual mannequin, but also make it possible for animation

application. For achieving this goal, the libraries of human skeleton frame called H-Anim 1.1 [24] which is performed by the Humanoid Animation Working Group is adopted to specify a standard way of representing humanoids. The human body consists of a number of segments (such as the forearm, hand and foot) which are connected to each other by joints (such as the elbow, wrist and ankle).

In H-Anim 1.1 format, the set of Joint nodes are arranged to form a hierarchy of human body and each segment is also have a number of site nodes, which define locations relative to the segment. The H-Anim 1.1 format not only provides a well tools and platform for humanoid designer, but also gives a practical skeleton frame for other approach with human body.

The body is typically built as a series of nested Joints, each of which may have a Segment associated with it. In H-Anim 1.1 organized human body structure, it totally has 94 skeleton joints, 15 skin parts (including head, right hand , right foot …etc), and 76 feature point. The feature points on the human body that defined in H-Anim 1.1 can be used for a variety of purposes.

Based on the H-Amin 1.1 architecture, we simplified Skeleton frame, which remained the critical joints that are the connect joints of limbs, of human body and denoted these joints as red solid ball in Fig. 2 (a). These joints which are elbow joints (the junction of upper arm and forearm), wrist joints (the forearm and hand), knee joints (the junction of thigh and shank), and ankle joint (the junction of shank and foot) are selected for segmentation of forearm region, upper arm region, thigh region, and calf region. The feature points displayed with blue solid ball in fig. 2 (b), cervicale, substernale, axilla, iliocristale, and crotch, are selected from the spec of H-Anim 1.1 and also used for segmentation.

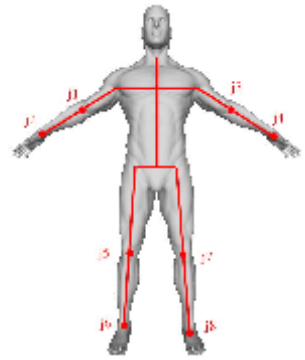

(a)

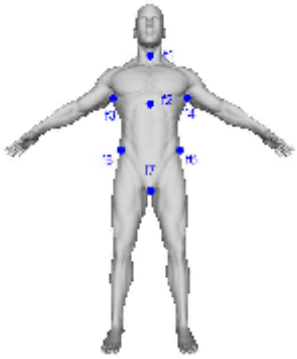

(b)

Fig. 2 The skeleton frame of human body (a) major joints and (b) feature points.

B. Segmentation

The Human body model segmentation process is not as simple as dividing human body into torso and limbs. The goal of this thesis is to create a mannequin based on the anthropometric measurement data. Each anthropometric measurement data is measured from the length or girth of each part of human body and represented its characteristic. Therefore, the deformation for creating a realistic virtual mannequin must be acted on each part with corresponding measurement data. In this thesis, the human body is divided into 11 parts (chest, waist, hip, right upper arm, right forearm, left upper arm, left forearm, right thigh, right calf, left thigh, and left calf) for deformation.

The individual difference of head is large, so it is not adopted for deformation. Oppositely, the individual difference of hand and foot are small, and therefore the hand and foot parts are not adopted for deformation. Fig. 3 illustrates the position of segmented parts on human body.

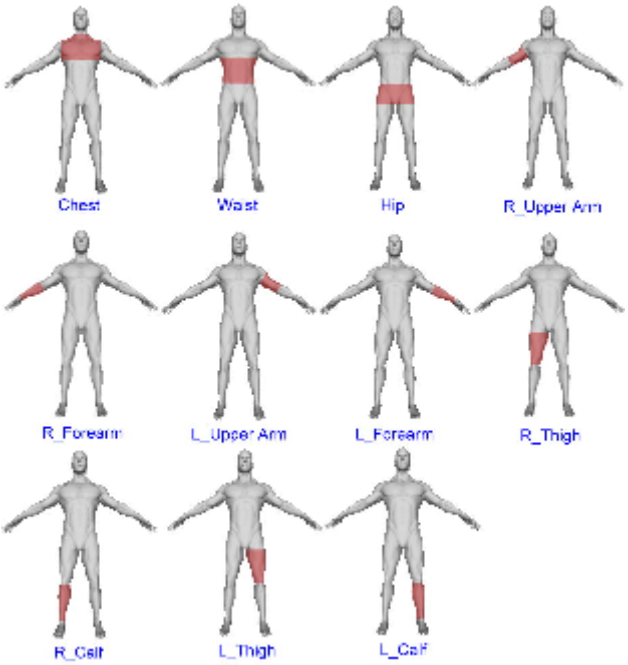

Fig. 3 Illustrates the position of segmented parts on human body.

The major joints and feature points which described on past section are all located at the significant position for body segmentation. The elbow joint is the connection of upper arm and forearm and used to construct the cutting plane C_{R_UF} (or C_{L_UF}) for separating. The wrist joint is the connection of forearm and hand and used to construct the cutting plane C_{R_FH} (or C_{L_FH}) for separating. The knee joint is the connection of thigh and calf and used to construct the cutting plane C_{R_TC} (or C_{L_TC}) for separating. The ankle joint is the connection of calf and foot and used to construct the cutting plane C_{R_CF} (or C_{L_CF}) for separating. Fig. 4 (a) illustrates the position of cutting plane belong to major joints.

The feature point cervicale is located around the middle of neck, so we can use this feature point to construct a cutting plane C_H for separating head part and torso part. The position of feature point substernale is located below the sternum and used to construct the cutting plane C_{CW} for separating the chest part and waist part. The feature point axilla is used to

construct the cutting plane C_{R_U} (or C_{L_U}) to define the upper bound of upper arm region.

The feature point iliocristale is the most lateral point on the iliac crest and adopted to construct the cutting plane C_{WH} for separating the waist part and hip part. The feature point crotch is used to construct the cutting plane C_{HT} for separating the hip part and thigh parts. Fig. 4 (b) illustrates the position of cutting plane belong to feature points.

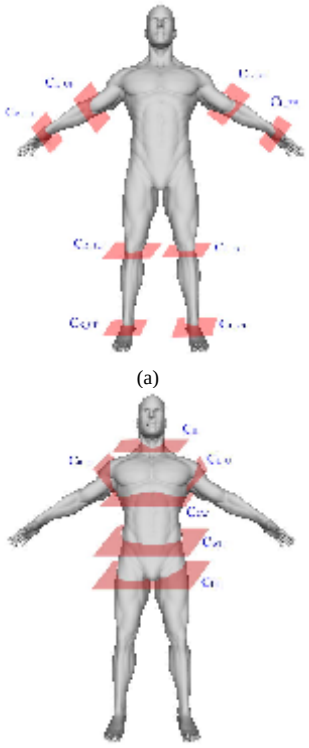

(a)

(b)

Fig. 4 Illustrates the position of cutting plane belong to (a) major joints and (b) feature points.

The definition and position of cutting planes for human body segmentation are preliminary explained on past paragraph, but the actual operation of human body model segmentation is involved. In addition, the major joints and feature point used for locating the position of cutting plane are need for marking manually.

The identification of each point, major joints and feature points, on human body model is handled by different principle, but the goal of these points are to construct the cutting plane for segmentation and make a connection link of neighbor parts by the corresponding nodes. Fig. 5 shows the entire link frame of human body model segment parts by using the connected nods and center axes which can also be seen as the skeletons of each part.

In the Fig. 5, it is easy and understandable for identifying some connect nods which are the major joints on H-Anim 1.1 system. There are five center axes, $Axis_{\_T}$, $Axis_{\_RA}$, $Axis_{\_LA}$, $Axis_{\_RL}$, and $Axis_{\_LL}$, in Fig. 5 and represent the torso and limbs (right arm, left arm, right leg, and left leg) respectively.

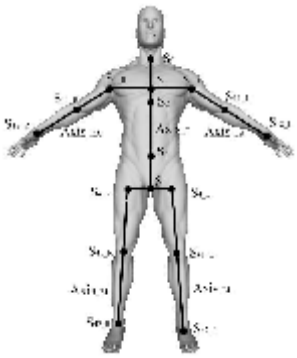

Fig. 5 Shows the linkages and nodes of entire human body segment parts.

C. Build Clustering

In this paper, we adopt the example based methodology for deformation; the created model is adjusted by the example model. So, the example model must be set or established before creating new model. If the build gap between example model and creating model is very large, the distortion of created model will be greatly. In order to address this problem, the available classification of human body build is adopted. It is not only preventing the excessive distortion due to the large gap of build, but also provides a characteristic deformation of each cluster.

The BMI factor which derived from anthropometric measurement; height and weight; and mentioned before is used to classify the build. The male builds are classified into six clusters with BMI (BMI<18.5, 18.5≦BMI< 22.5, 22.5≦ BMI< 25, 25≦BMI<28, 28≦BMI<31.5, and BMI≧31.5), and the female builds are also classified into six clusters with BMI (BMI<15, 15≦BMI< 17.5, 17.5≦ BMI< 19, 19≦ BMI<22, 22≦BMI<26.5, and BMI≧26.5) respectively.

In this approach, sixty human body models are selected from TAIBBK database, which is the 3-D human body scanning data is the body digitalized data, and the slice data can be extracted with the plane which is concerned. The Taiwan human body bank (TAIBBK) [25][26], which stands for Industrial Technology Research Institute, Tshing Hua University, and Chang Gung University, is a large scale 3-D anthropometric measurement project. About 1100 civilians, between the age of 19 and 65 in Taiwan, were scanned, for radius distance deformation training and each cluster has allocated five models. These selected models are close to uniform distribution in the BMI interval of each cluster, and therefore theses models can be represented of each cluster sufficiently.

III. Radius Distance Deformation

The Radius Distance deformation system is a cylinder coordinate system and contains with the orientation vertex and control points. As the same with other deformation algorithm, the 3-D object is deformed through the manipulation the control points which are underlying the object. In generally, the arrangement of control point is lattice model, and the extendedly definition of lattice is transferred from cubic (or rectangular) to cylinder. Through of this transferred, the adaptability of deformation application will be more wildly especially in human body model.

D. Structure

Cylindrical coordinate system is a generalization of two dimensional polar coordinates to three dimensions by superposing a height z axis and notation as (r,θ,z). The radial (r) coordinate is the scalar of shortest Euclidean distance between the vertex and z axis, and the azimuthal coordinate (θ) is an angular measurement in aspherical coordinate system and to measure the angle between the projected vector ($\vec{r}$), is the perpendicular project vector of vector ($\vec{s}$) from origin to vertex, and x-axis on the x-y plane. The Fig. 6 illustrates the cylinder coordinate system.

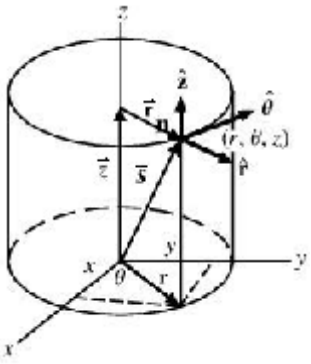

Fig. 6 Illustrate the cylinder coordinate system.

For simplified calculation, the movement of vertex is defined for moving along the direction of vector ($\hat{r}$) in radius distance deformation system. The vertex $\hat{r}$ is the unit vector of radial vector $\vec{r}$ and can be show in rectangular coordinate system as:

$$\hat{r} = \frac{\vec{r}}{\vec{r}} = \frac{x\hat{x} + yy}{\vec{r}} = x\cos\theta + y\sin\theta. \qquad (1)$$

In this approach, we propose an extended radius distance deformation method with using a constrain region instead of a constraint control point. The novel deformation function for simplify the position calculation is also present in our approach. The radius distance coordinate system contained with the scalar distance between a point and origin (or center) and the azimuth angle between the reference direction and the line from the origin is applied. Fig. 7 is illustrated the extended lattice arrangement of the vertex and control points in cylinder coordinate system with Radius Distance Free Form Deformation.

In fig. 7, there are s layers of deformation control (blue circles) and the control point (blue solid circle) are unified distribute with the fixed angle which determinates from the number of control point in a control plane, between the neighbors on the circle contour in each layer. The control point P_{ij} is defined as the i-th layer and at the j-th control point. In our approach, the number of control point on each layer is set for 8 points and the cross section point of contour and y axis is assigned for P_{i0}. The radius distance of each control layer is defined as R and the distance between each layer is fixed as h, so the height H of local deformation part is $(s\text{-}1)h$. The slices of object are show as red solid circles and the vertexes are denoted as solid red circle. The radius distance r_{pq} of vertex v_{pq} is defined as the distance between the point c_p, which is the cross section point of axis and slice, and vertex v_{pq}. The control lattice is constructed by stacking up the plane of control points and the shape of object is also constructed by stacking up the plane of vertex and displayed with red color curve. The structure constructed by stacking up the parallel slice which can be seen as the cutting contour of object shape, is called sweep-based model.

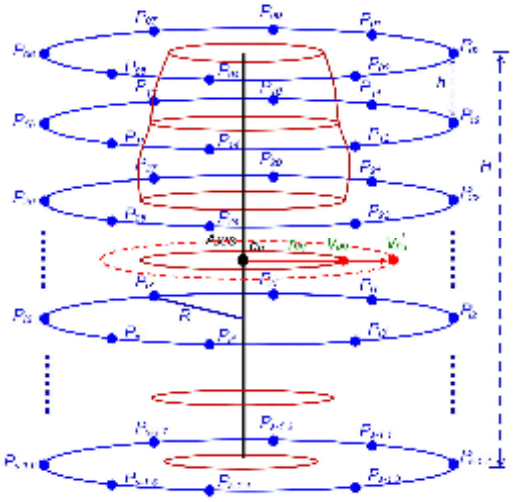

Fig. 7 Illustrate the structure of radius distance deformation with sweep-based model.

In sweep-based model, the object was cut into n slices and the vertex v_{oq} belong to these slice is denoted as the p-th layer and q-th vertex. The point v_{oq} in cylinder coordinate can be written as:

$$\begin{aligned} v_{pq} &= (r_{pq}, \theta_q, h_p) \\ &= (r_{pq}, \frac{2q}{m}\pi, p*h) \quad p \in [0, n-1] \ \ \& \ q \in [0, m-1] \end{aligned} \qquad (2)$$

where m is the number of chosen vertexes in p-th layer.

E. Radius Distance Deformation

In this paper, we take the radius distance deformation model and 3-D scanning model from database for repetition training to obtain the correlations function of vertex and control points. The relations of each vertex and control point are very complicated and the calculations of movement are the heavy task. To simplify the architecture of radius distance deformation model is the feasible way to reduce the computing load. At first, the movements of each vertex or control point are restricted along the direction of radial vector which has been described before.

The other way for simplified calculation is to reduce the sampling rate of vertex chosen on slice contour for calculating the influence on control point. The determination of vertex sampling rate is a trade off problem. For keeping the details of shape, the sampling rate will not take to low, but the computing load will increase very slope. Oppositely, low sampling rate of vertex used will effective reduce the computing load, but some details of shape will lost. If the sampling way is consider as the same as the arrangement of control point on the control plane. It is not only efficiently

reduce the calculation, but also make it more easy to indicate the relation of vertex and control point.

The chosen of vertex locate on the slice contour is defined to tkae the same azimuth angle with control point. So the number of chosen vertex in each sweep layer is also 8 in training model. Fig. 8 shows the *p*-th slice contour and *i*-th control plane and designated as red and blue circles respectively. The inner red circle is denoted as the slice contour of example model and outer circle is denote as the contour of training model, and then the movement vector $\vec{\delta}_{v_{pq}}$ of vertex v_{pq} can be calculated as:

$$\vec{\delta}_{v_{pq}} = v'_{pq} - v_{pq} = (r'_{pq} - r_{pq}) \vec{u_q} \Big/ |\vec{u_q}| \tag{3}$$

where $\vec{u_q}$ is the unit vector of *q*-th direction.

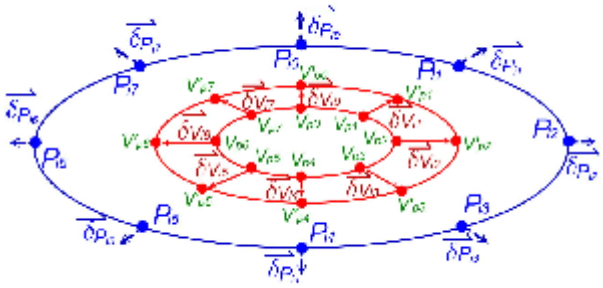

Fig. 8 Illustrate the arrangement of vertex on *p*-th object slice contour and control points on *i*-th control plane.

The goal of repetition training procedural is to receive the correlation of vertex and control point. As mentioned before, the build, male and female, are separated into six clusters, the training processes are repeated in each cluster. Moreover, the each segment parts of human body model are still done respectively.

In training model, the function of control point P_{ij} movement is defined as:

$$\begin{aligned} \vec{\delta}_{P_{ij}} &= \sum_{p=0}^{n-1}\sum_{q=0}^{m-1} f(v_{pq}) = \sum_{p=0}^{n-1}\sum_{q=0}^{m-1} D_{ij}(p,q) E_{ij}(p,q) * \vec{u}_j \\ &= (C_r - 1) a_{ij} e^{|1-C_r|} * \vec{u}_j \end{aligned} \tag{4}$$

where $D_{ij}(p,q)$ is a volume of the distance ratio of vertex v_{pq} to control point P_{ij} and can be written as :

$$D_{ij}(p,q) = 1 - \frac{d(v_{pq}, P_{ij})}{D_{\max}} \tag{5}$$

where $d(v_{pq}, P_{ij})$ is the distance between v_{pq} and P_{ij} and can be denoted as follow

$$\begin{aligned} d(v_{pq}, p_{ij}) = [&(R\sin\theta_j - r_{pq}\sin\theta_q)^2 + (R\cos\theta_j - r_{pq}\cos\theta_q)^2 \\ &+ ((i-1)h - (p-1/n-1)H)^2]^{1/2}. \end{aligned} \tag{6}$$

The formula $E_{ij}(p,q)$ is the effective component of vertex v_{pq} to control point P_{ij}, hence the $E_{ij}(p,q)$ can be explained for the inner product of the vector of vertex v_{pq} movement to the unit vector of control point P_{ij}. The formula $E_{ij}(p,q)$ is showed as:

$$E_{ij}(p,q) = \vec{\delta}_{v_{pq}} \bullet \vec{u}_{ij} = (v'_{pq} - v_{pq}) \bullet \vec{u}_j \tag{7}$$

where $\vec{\delta}_{v_{pq}}$ is delta vector of vertex v_{oq} from standard model contour to trainning model contour. $\vec{u}_j$ is the unit vector of *j*-th control point. In the equation (4), *f* is deformation function where $f : R^3 \to R^3$ and a_{ij} is the free form deformation parameter set of control point P_{ij}. C_r is the circumference ratio of standard model and training model, and defined as:

$$C_r = L / L_{std} \tag{8}$$

where *L* is the circumference of training, and L_{std} is the circumference of standard model.

The parametric set *A* of control point can be acquired from (4) and be denoted as:

$$P = L(C_r) * A * U = (C_r - 1) e^{|1-C_r|} * A * U \tag{9}$$

where *U* is the unit vector set of each orientation.

IV. Extended Cylinder Free Form Deformation

Free Form Deformation is an important geometric shape modification method in computer graphics and also the very intuitive modeling technique. To deform the object, the user first deforms the embedding space; then the deformation is passed to the object. If the relation function of anthropometric measurement and the movement of control points is acceptable, the realistic virtual human body model can be created by free form deformation.

A. Free Form Deformation

All the space deformation methods mentioned before are independent of the geometric representation. Theoretically, the deformation should be act on every point (or vertex) on object. The free form deformation method consists of embedding the geometric model or region of the model that has to be deformed in to a parallelepipedical 3-D lattice.

In our implementation, the 3-D cylinder lattice is represented by a tensor product piecewise tri-cubic Bezier curve. Fig. 9 illustrates one control plane structure of extended free form deformation system. The control plane is located at the plane of Z= z, and eight control points are indicated as red solid circle. The vertex displayed in blue solid circle is located at the position (r, θ, z) in cylinder coordinate. The dotted square which covered control plane contour, and four corners is display as hollow circle.

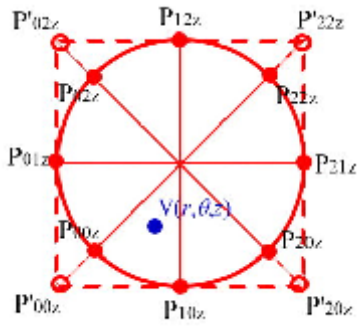

Fig. 9 Illustrate the arrangement of control points on control plane.

For simplifying the formulae of deformation, we modified the rectangular lattice to approximate the cylinder lattice in this approach. The standard free form deformation implements the 3-D lattice by a tensor product. The rectangular coordinate system is well used in normalized function which is for bounding the object in free form deformation. If control points (p_{00z}, p_{02z}, p_{20z}, and p_{22z}) are considered as the point of corners (p'_{00z}, p'_{02z}, p'_{20z}, and p'_{22z}) on rectangular, the normalized functions of rectangular coordinate system can be used in this approach. So the normalized function of cylinder free form deformation can be expressed as:

$$s = \frac{\vec{Z}\times\vec{T}\cdot(x-x_0)}{\vec{Z}\times\vec{T}\cdot\vec{S}}$$
$$t = \frac{\vec{S}\times\vec{Z}\cdot(y-y_0)}{\vec{S}\times\vec{Z}\cdot\vec{T}} \qquad (10)$$
$$z = \frac{\vec{T}\times\vec{S}\cdot(z-z_0)}{\vec{T}\times\vec{S}\cdot\vec{Z}}$$

Where (x_0, y_0, z_0) is the origin point of this box, and (x, y, z) is the scalar value of vertex v in rectangular coordinate.

The position of vertex $v(r,\theta,z)$, underlying deformation control plane, after deformation is defined as:

$$v_{def}(s,t,z) = \sum_{i=0}^{2}\sum_{j=0}^{2}\sum_{k=0}^{n-1} B_i(s)B_j(t)B_k(z)P_{ijk} \qquad (11)$$

Where $p_{ijk} \in R^3$ is the control point, B_i(s) are the degree 3 Berstein polynomials, and n is the number of control plane. So the formulae (10) can be expressed as:

$$\begin{aligned} v_{def}(s,t,z) &= \sum_{i=0}^{2}\sum_{j=0}^{2}\sum_{k=0}^{n-1} B_i(s)B_j(t)B_k(z)P_{ijk} \\ &= \sum_{i=0}^{2}\binom{2}{i}(1-s)^{2-i}s^i\left(\sum_{j=0}^{2}\binom{2}{j}(1-t)^{2-j}t^j \right. \\ &\qquad \left.\left(\sum_{k=0}^{n-1}\binom{n-1}{k}(1-z)^{n-1-k}z^k P_{ijk}\right)\right) \end{aligned} \qquad (12)$$

After each parts of human body model are deformed through the anthropometric measurement by extended free form deformation, the rough model of realistic virtual human body model will already finished.

B. Smoothing

The part by part deformations of human body model will product the blank and rough body model. The Deforming a segment part without any filtering stage will result in discontinuous surface passed at the boundaries of the parts. To deal with this problem, we adopt the filtering over the final displacement vectors.

The window filter is a mathematical function that is zero-valued outside of some chosen interval. For instance, a function that is constant inside the interval and zero elsewhere is called a rectangular window.

On each segment part, we applied the Tukey windows [27] as the smoothing window function with different parameters. The Tukey window is as called tapered cosine window and smoothly decay the displacement value on the boundaries of segment part to zero. The Tukey window function is defined by:

$$Q(u) = \begin{cases} \frac{1}{2}\left\{1+\cos\left(\frac{2\pi}{\alpha}\left[u - N\frac{\alpha}{2}\right]\right)\right\} & 0 \le u < N\frac{\alpha}{2} \\ 1.0 & N\frac{\alpha}{2} \le u < N(1-\frac{\alpha}{2}) \\ \frac{1}{2}\left\{1+\cos\left(\frac{2\pi}{\alpha}\left[u - N + \frac{\alpha}{2}\right]\right)\right\} & N(1-\frac{\alpha}{2}) \le u \le N \end{cases} \qquad (13)$$

where N is number of vertex space on z axis for boundary smoothing, $Q(u)$ is the corresponding adjustment value on radial coordinate scale. The scalar u is normalized local coordinate value, and can easy be found by using linear algebra. The local coordinate normalized function is defined as:

$$u = \frac{z - z_{\min\_sr}}{z_{\max\_sr} - z_{\min\_sr}} \qquad u \in [0,1] \qquad (14)$$

where z is the scale of z coordinate, Z_{max_sr} and Z_{min_sr} are the maximum scale and minimum scale of z coordinate of smoothing region.

The parameter α is the window shape adjustment and determines the ratio of taper on constant sections. So the parameter of window function is depending on the deforming amplitude of boundary region. In intuitive observation, the big volume parts will need to use the large window for filtering, oppositely, the small volume parts will need to use the small window for filtering.

V. IMPLEMENTATION

In this section, we implement a framework where the above mentioned techniques are applied on the all anthropometric measurement acquirable. The required measurement data are (chest, waist, hip, left upper arm, left forearm, right upper arm, right forearm, right thigh, right calf, left thigh, and left calf) manual measured. The prior process is to cluster the displacement models.

Our implementation platform is a personal computer based with 2.4GHz pentium4 cpu, 4G memory ram, NVIDIA GeForce FX5900 GPU graphic card, and Microsoft window xp operation system. The deformation algorithm is written in C++ and OpenGL.

The Implementation will create and display 3 demo models, two male and one female, each model are not in the same cluster. The prior manual measured data are show above the displacement figure.

Table I

THE ANTHROPOMETRIC MEASUREMENT DATA OF EXAMPLE MODEL AND CREATED MODEL I.

	Height	**Weight**	**BMI**	**Cluster**	**R. upper arm**
Example	172	74.8	25.28	M_4	31.5
Created	174	78.4	25.89	M_4	32
	R. fore arm	**L. upper arm**	**L. fore arm**	**Chest cir.**	**Waist cir.**
Example.	29	31.4	29.4	94.3	91.2
Created	29.5	31.8	29.9	97.2	92.3
	Hip cir.	**R. thigh**	**L. thigh**	**R. shank**	**L. shank**
Example.	99.2	52.6	52.4	39.5	39
Created	99.7	53.2	53	41	41.5

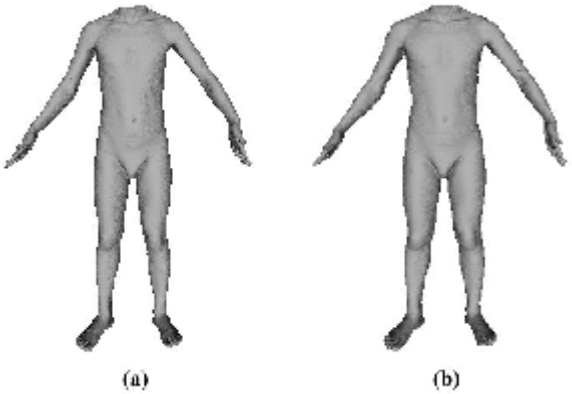

Fig. 10 Display the demo model I (a) the example model and (b) The created virtual mannequin

Table II

THE ANTHROPOMETRIC MEASUREMENT DATA OF EXAMPLE MODEL AND CREATED MODEL I.

	Height	**Weight**	**BMI**	**Cluster**	**R. upper arm**
Example.	175	90.3	29.48	M_5	34.4
Created	178	91.5	28.88	M_5	33.6
	R. fore arm	**L. upper arm**	**L. fore arm**	**Chest cir.**	**Waist cir.**
Example.	30.8	34.1	30.6	105.2	104.2
Created	30.7	33.6	30.3	99.8	101.3
	Hip cir.	**R. thigh**	**L. thigh**	**R. shank**	**L. shank**
Example.	108.2	56.1	55.1	44..1	43.3
Created	105.7	53.2	54.8	43.2	43.0

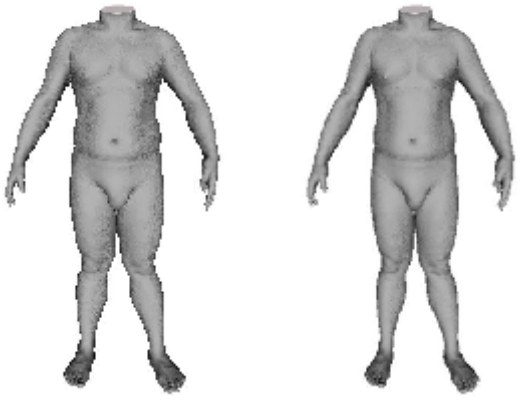

Fig. 11 Display the demo model II (a) the example model and (b) The created virtual mannequin

Table III

THE ANTHROPOMETRIC MEASUREMENT DATA OF EXAMPLE MODEL AND CREATED MODEL I.

	Height	**Weight**	**BMI**	**Cluster**	**R. upper arm**
Example.	158	47.1	18.87	F_3	28.8
Created	162	47.5	18.10	F_3	27.7
	R. fore arm	**L. upper arm**	**L. fore arm**	**Chest cir.**	**Waist cir.**
Example.	23.6	28.4	23.4	87.3	90.2
Created	23.3	27.6	22.9	87.2	89.3
	Hip cir.	**R. thigh**	**L. thigh**	**R. shank**	**L. shank**
Example.	93.2	47.6	48.1	37.5	38
Created	90.7	45.9	46	36.2	36.5

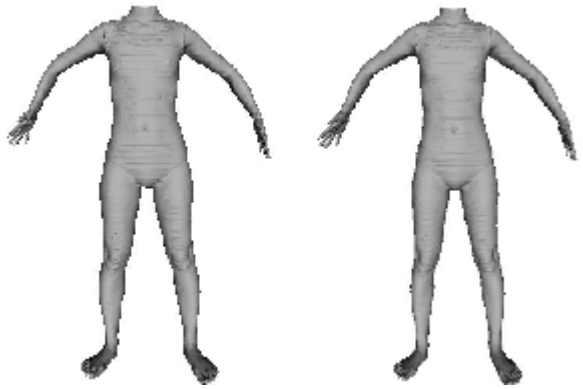

Fig. 12 Display the demo model III (a) the example model and (b) The created virtual mannequin

VI. CONCLUSIONS

In this paper, we introduce an example based approach to create a realistic virtual human body model through the anthropometric measurement. The human body skeleton frame is taken for construct the linkage of whole human body, and also provides the connection node for each separated parts. The radius distance deformation method is propose to seek the relation function of vertex and control point on cylinder coordinate system taking the human model from TAIKBB database. The extended cylinder free form deformation provides a good method to multiple the 3-D objects, such as deformation, translate, rotation, bending, twisting …etc. The cooperation of radius distance deformation method and extended free form deformation is not only provide a well used system to create the realistic human body model, but also can use this created model to edit humanoid animations more easy the other object structure.

Although the realistic humane body can be created by use this approach, there are still have some challenges need to take. The human head deformation is a big challenge to deal with the complex shape of human face, and how to preserve the details of body skin such as wrinkle and fineness concave is another task need to deal in the future work.

REFERENCES

[1] J. A. Roebuch, Jr., Anthropometric Methods: Designing to Fit the Human Body. Santa Monica, CA: Hum. Factors and Ergonom. Soc., 1995.
[2] (2002) Human Solutions website. [Online]. Available: http://www.human-solutions.com/apparel/technology_scanning_en.php
[3] C. C. Gordon, T. Churchill, C. E. Clauser, B. Bradtmiller, J. T. McConville, I. Tebbetts, and R. A. Walker, 1988 anthropometric survey of US army personnel: methods and summary statistic. NATICK/TR-89/044. US Army Natick Research, Development, and Engineering Center, Natick, MA, 1989.
[4] K. Robinette, H. Daanen, and E. Paquet, "The CAESAR project: A 3-D surface anthropometric survey," 2nd Int. Conf. on 3-D digital imaging and modeling, Ottawa, Ont. , Canada, pp. 380-386, October 1999.
[5] (2009) The HumanBody 3D Website. [Online]. Available: http://www.humanbody3d.com/
[6] (2006) The tutorialsphere Website. [Online]. Available: http://www.tutorialsphere.com/tutorials/maya-3d/modeling
[7] E. Paquet and H. L. Viktor, "Adjustment of virtual mannequins through anthropometric measurements, cluster analysis, and content-based retrieval of 3-D body scans," IEEE Trans. on Instrumentation and Measurement, vol. 56, pp.1924 - 1929, October 2007.
[8] El-Hakim, Gruen, Walt on, Santa Clara ,3D Reconstruction of Static Human Body with a Digital Camera, Videometrics VII, SPIE Electronic Imaging, Vol. 5013, pp. 38-45, USA, January 2003.
[9] In Luc Van Gool, Human Body Reconstruction from Image Sequences, Pattern Recognition (DAGM 2002), Lecture Notes in Computer Science 2449, Springer 2002, pp. 50-57, Zurich, Switzerland, September 2002.
[10] Fabio Remondino, 3D Reconstruction of Static Human Body with a Digital Camera, Videometrics Conference, SPIE Proc, pp. 38-45, 2003.
[11] A. Barr. Superquadrics and angle-preserving transformations. IEEE Computer Graphics and Applications, Vol. 1(1), PP. 11–23, 1981.
[12] F. Scheepers, R. E. Parent, W. E. Carlson, and S. F. May. Anatomy-based modeling of the human musculature. In SIGGRAPH '97: Proceedings of the 24th annual conference on Computer graphics and interactive techniques, pp. 163–172, New York, NY, USA, 1997. ACM Press/Addison-Wesley Publishing Co.
[13] T. W. Sederberg and S. R. Parry. Free-form deformation of solid geometric models. In SIGGRAPH '86: Proceedings of the 13th annual conference on Computer graphics and interactive techniques, pages 151–160, New York, NY, USA, 1986. ACM Press.
[14] J. E. Chadwick, D. R. Haumann, and R. E. Parent. Layered construction for deformable animated characters. In SIGGRAPH '89: Proceedings of the 16th annual conference on Computer graphics and interactive techniques, pp. 243–252, New York, NY, USA, 1989. ACM Press.
[15] S. Coquillart. Extended free-form deformation: a sculpturing tool for 3d geometric modeling. In SIGGRAPH '90: Proceedings of the 17th annual conference on Computer graphics and interactive techniques, pp. 187–196, New York, NY, USA, 1990. ACM Press.
[16] M. Grosso, R. Quach, E. Otani, J. Zhao, S.Wei, P. Ho, J. Lu, and N. Badler. Anthropometry for computer graphics human figures. 1987.
[17] F. Azuola, N. Badler, P. Ho, I. Kakadiaris, D. Metaxas, and B. Ting. Building anthropometry-based virtual human models. Proc. IMAGE VII Conference, June 1994.
[18] S. Jianhua, N. Magnenat-Thalmann, and D. Thalmann. Human skin deformation from cross-sections. In Computer Graphics Int. '94, 27-1 1994.
[19] J. Shen and D. Thalmann. Interactive shape design using metaballs and splines. In Implicit Surfaces'95, pp. 187–196, Grenoble, France, 1995.
[20] N. H., H. M., K. T., K. T., S. I., and O. K. Object modeling by distribution function and a method for image generation. Transaction for the Institute of Electronics and Communication for Engineers of Japan, J68-D:718–725, 1985.
[21] D.-E. Hyun, S.-H. Yoon, M.-S. Kim, and B. Jittler. Modeling and deformation of arms and legs based on ellipsoidal sweeping, In PG '03: Proceedings of the 11th Pacific Conference on Computer Graphics and Applications, page 204, Washington, DC, USA, 2003. IEEE Computer Society.
[22] D.-E. Hyun, S.-H. Yoon, J-W Chang, J-K Seong, M-S Kim and B. Jüttler, Sweep-based human deformation, in Special Issues of Pacific Graphics 2005, Vol. 21, No. 8-10, pp. 542-550, 2005.
[23] W. Zhaoqi, M. Tianlu, and X. Shihong. A fast and handy method for skeleton-driven body deformation. Comput. Entertain., vol.4, no. 4, pp. 6, New York, NY, USA, 2006.
[24] (2006) The humanoid Animation Working Group Website. [Online]. Available: http://www.h-anim.org/
[25] (2002) Taiwan Human Body Bank (TAIBBK) website [Online]. Available:,http://3d.cgu.edu.tw/DesktopDefault.asp,
[26] C. Y. Yu, Y. H. Lo and W. K. Chiou, "The 3D scanner for measuring body surface area: a simplified calculation in the Chinese adult," Applied Ergonomics, Vol.34, pp.273-278, 2003.
[27] Tukey, J.W. . "An introduction to the calculations of numerical spectrum analysis". Spectral Analysis of Time Series, pp.25–46,1967.
[28] F. J. Harris, "On the use of windows for harmonic analysis with the discrete Fourier transform," Proceeding of the IEEE, vol. 66, pp. 51-83, 1978.

Sheng-Fuu Lin was born in Tainan, R.O.C., in 1954. He received the B.S. and M.S. degrees in mathematics from National Taiwan Normal University in 1976 and 1979, respectively, the M.S. degree in computer science from the University of Maryland, College Park, in 1985, and the Ph.D. degree in electrical engineering from the University of Illinois, Champaign, in 1988. Since 1988, he has been on the faculty of the Department of Electrical and Control Engineering at National Chiao Tung University, Hsinchu, Taiwan, where he is currently a Professor. His research interests include image processing, image recognition, fuzzy theory, automatic target recognition, and scheduling.

Shih-Che Chien was born in Chiayi, R.O.C., in 1978. He received the B.E. degree in electronic engineering from the Nation Chung Cheng University, in 2002. He is currently pursuing the M.E. and Ph.D. degree in the Department of Electrical and Control Engineering, the National Chiao Tung University, Hsinchu, Taiwan. His current research interests include image processing, image recognition, fuzzy theory, 3D image processing, intelligent transportation system, and animation.